Intrinsic attenuation: removing the stratigraphic effect from attenuation measures

Gary F. Margrave, Sylvestre Charles (Suncor), and Hossein Aghabarati (Suncor)

SUMMARY

Estimates of attenuation computed from seismic data are inherently composed of two parts: a local intrinsic effect, and a nonlocal stratigraphic effect. The former is a property of the rock that the wave is transiting through and represents actual loss of wave energy to heat. The latter is a wave interference due to the cumulative effect of short path multiples occurring along the transmission path. It is often desirable to estimate intrinsic attenuation as a reservoir parameter as it may indicate reservoir quality. However, attenuation measurements from seismic data will always consist of both intrinsic and stratigraphic effects so the isolation of the former requires the estimation of the latter. We investigate the possibility of using a visco-acoustic 1D synthetic VSP driven by finely sampled well information to estimate the stratigraphic attenuation. We then use these estimates to isolate the intrinsic attenuation from a zero offset VSP. We show that well-log sampling of 0.3048m in depth is sufficient to estimate the stratigraphic effect; however, the unavoidable occurrence of an unlogged overburden means that the magnitude of the estimate will always be too small. The estimates of total attenuation on a real VSP are made on the separated downgoing wavefield. Intrinsic attenuation then follows by subtracting the stratigraphic component, estimated from the synthetic VSP, from the measured total attenuation. Our estimates of intrinsic attenuation fail to show the theoretically expected monotonically increasing behaviour. Among the possible reasons for this are the imperfect nature of VSP wavefield separation, problems with receiver and sonic coupling in the borehole, the aforementioned unlogged overburden, and mode-converted scattered waves that are not included in the visco-acoustic approximation. These are topics for future research.

INTRODUCTION

We present a study of the measurement of seismic attenuation with particular attention paid to the possibility of separating the measured attenuation into stratigraphic and intrinsic components. Stratigraphic attenuation, also known as stratigraphic filtering, was introduced to geophysics by O'Doherty and Anstey (1971). They showed that a finely layered perfectly elastic medium will exhibit an apparent attenuation that during measurement is essentially indistinguishable from true intrinsic attenuation. At the mineral grain level the processes are clearly distinct with intrinsic attenuation being attributed to internal friction losses to heat as the rock vibrates in response to a seismic wave. Intrinsic attenuation manifests as an exponential attenuation of higher seismic frequencies with an associated minimum-phase rotation. On the other hand, stratigraphic attenuation is only an apparent loss in which the higher frequencies are progressively delayed as they reverberate through the finely layered sequence. If one were to record long enough and with very great precision, there would be no energy loss due to stratigraphic filtering, only energy delay. However, in any practical setting, O'Doherty and Anstey showed that the stratigraphic filtering effect is also an exponential attenuation with minimum-phase rotations just like intrinsic attenuation. It follows that a finely-

layered visco-elastic system, which is a good model for a real sedimentary sequence, will show an attenuation that is a combination of the two effects.

From an exploration perspective, it is desirable to separate an attenuation measurement into intrinsic and stratigraphic components. This is because only the intrinsic component can be considered as a reservoir property that may indicate conditions of economic interest. We consider the measurement of total (or effective) attenuation in a VSP (vertical seismic profile) experiment conducted in a well where good logging information is also available. Using the logging information, we create a synthetic VSP incorporating all of the stratigraphic detail in the logs. From this synthetic VSP, stratigraphic attenuation can be directly measured because intrinsic attenuation is prescribed and therefore known. While this seems inherently feasible, matters are complicated because the synthetic VSP must be created from an earth model containing a thousand or more layers and it must have a physically accurate response at high frequencies. Moreover, the well logs must be provide a complete description of the elastic properties of the stratigraphy and must extend essentially from surface to the reservoir target. Additionally, the real VSP must be of high quality and the wavefield separation, required to isolate the downgoing direct wave upon which attenuation measures are conducted, must be very accurate. These conditions are extremely demanding and we have only partially met them.

The setting for our experiment is in northern Alberta at a site associated with the oil sands and owned and operated by Suncor. The VSP was acquired by a 3rd-party contractor using a special receiver tool that allowed the deployment of 3C accelerometer sensors at 1m intervals from surface casing to the reservoir at some 340m depth. The source as a small, 1/8 kg, dynamite charge placed 6m deep and 5m from the well head resulting in a nearly zero-offset VSP. Available well logs were acquired before the VSP and are p-wave sonic and density. For both, the upper 15m of the borehole were not logged. Also problematic is that the upper 150m of the p-wave sonic were not directly measured but rather synthesised from the measured density log. There was no s-wave log available.

Our synthetic VSP was constructed using a visco-acoustic algorithm and not a visco elastic one. We did not have a visco-elastic code available that we felt could handle a thousand layers and moreover we did not have s-wave velocity information.

We begin with a discussion of stratigraphic attenuation and its estimation. We discuss the creation of a synthetic visco-acoustic VSP and show detailed results from earth models with various levels of stratigraphic detail. We then describe two alternative methods of measuring attenuation and compare their relative merits. We also describe the attenuation attribute called *cumulative attenuation*, or CA, and compare it to the more conventional measurement of the rock property Q. Next, we show estimates of stratigraphic attenuation and show that it can be quite significant accounting for 40% or so of the total attenuation. Finally we consider the real VSP and show the results of our attempts to correct real attenuation measures. In our concluding remarks we discuss the mixed success of our results and comment on how to improve things in a future experiment.

ESTIMATING STRATIGRAPHIC ATTENUATION

The sonic and density logs used in this study were resampled at $\Delta z = 0.0508$m and are shown in Figure 1. However, these logs were acquired with a field sample size of $\Delta z = 0.3048$m (or 1 ft), which is common for western Canada, so the resampling is 6 times finer than the acquisition sampling. As will be seen, this resampling does not provide any additional stratigraphic attenuation. Both logs appear to begin at 15m depth extend to just under 340 m depth; however, above 150m, the p-wave sonic is actually artificial having been generated from the density log. Additionally, the p-wave sonic has been calibrated to give first-break traveltimes in agreement with observed VSP times.

Previously (Margrave, 2014a), it has been found that the simulation of a 1D VSP using well log measurements and a plausible intrinsic Q model allows the stratigraphic attenuation to be estimated. Figure 2 is taken from that paper and shows the results of a series of experiments conducted at different blocking sizes designed to estimate Q_{bias} which is defined as the difference between the average measured Q ($Q_{apparent}$) and the average intrinsic Q or $Q_{bias} = \bar{Q}_{apparent} - \bar{Q}_{intrinsic}$ where the overbar indicates averaging. As can be seen, the Q_{bias} is only meaningfully greater than 0 (indicating a significant stratigraphic effect) when the blocking size is less than 10m.

We follow that approach here using the algorithm described by Ganley (1980) and Margrave (2014b) to simulate a 1D VSP in a finely layered medium where each layer has a unique value of velocity, density and Q. Given well logs so finely sampled as ours, we can block the logs into coarser layers of any desired thickness using Backus averaging of parameters while retaining the original sample rate. Thus, if we choose a block thickness of 5m, then each layer will have $5/\Delta z \approx 98$ samples with the same constant value. Figure 3 shows the results of 4 different blockings of the original logs into layers of thicknesses of 0.05m, 0.3048m, 5m, and 15m. These blocking sizes where chosen with consideration of the results shown in Figure 2 such that we expect a strong stratigraphic effect for the first two, a reduced effect for the third, and no effect for the fourth. In these blockings, a plausible overburden has been attached to define the unlogged upper 15m and an empirical intrinsic Q model has been computed using the method of Margrave (2013). Thus each of these four different blocking represents an alternative 1D earth model based of the original well logs of Figure 1. All four models have the same internal sample rate of 0.05m but they have drastically different levels of stratigraphic detail.

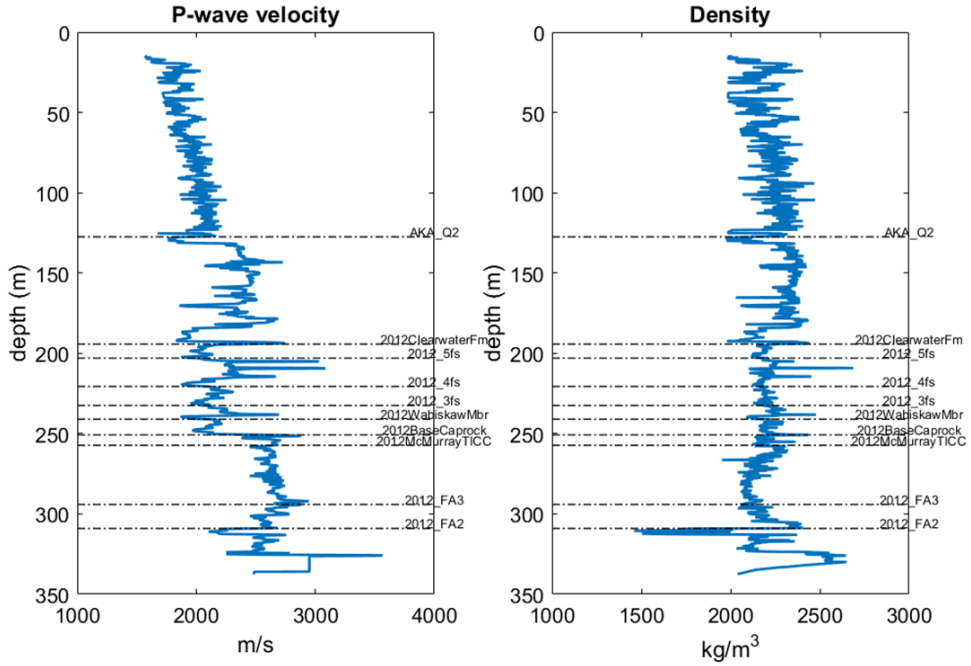

Figure 1: The sonic (left) and density (right) logs used in this study. The sonic log is display in velocity units rather than slowness. The logs are sampled at Δz=0.0508 m and extend to a depth of just under 340m.

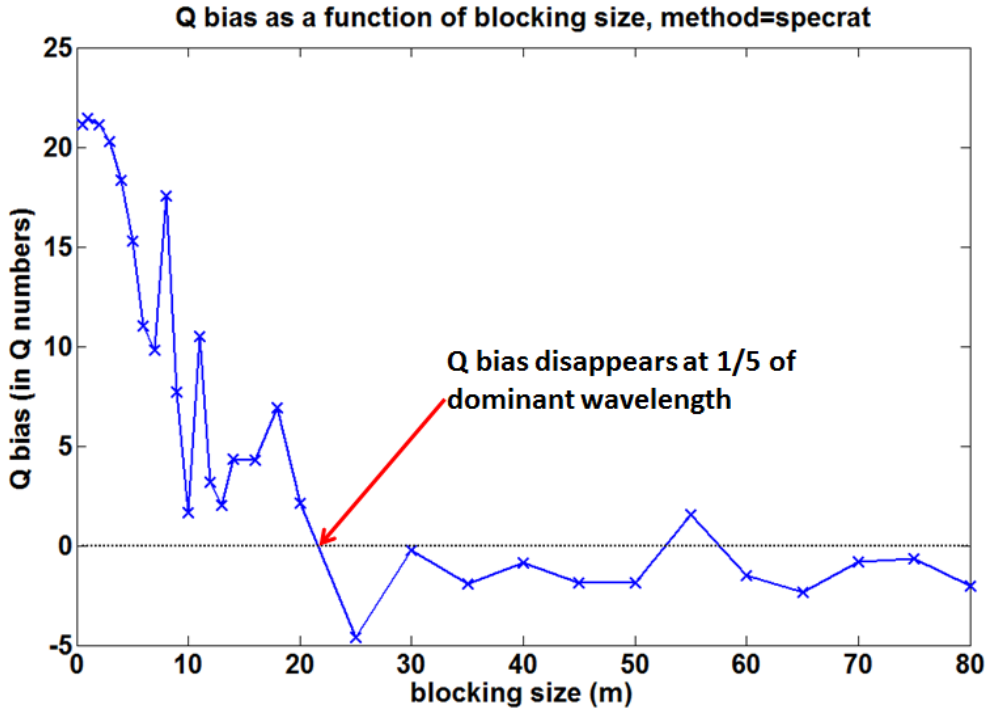

Figure 2: (From Margrave (2014)). The results of an experiment using different log blocking sizes and then measuring the apparent Q when the intrinsic Q is known. The Q_{bias} is defined as the difference between the average apparent Q and the average intrinsic Q, or $Q_{bias} = \bar{Q}_{apparent} - \bar{Q}_{intrinsic}$ where the overbar indicates averaging. Positive Q_{bias} indicates that there is a significant stratigraphic effect and this is indicated for blocking sizes of 10m and less. Above 10m the bias is essential zero to within experimental accuracy.

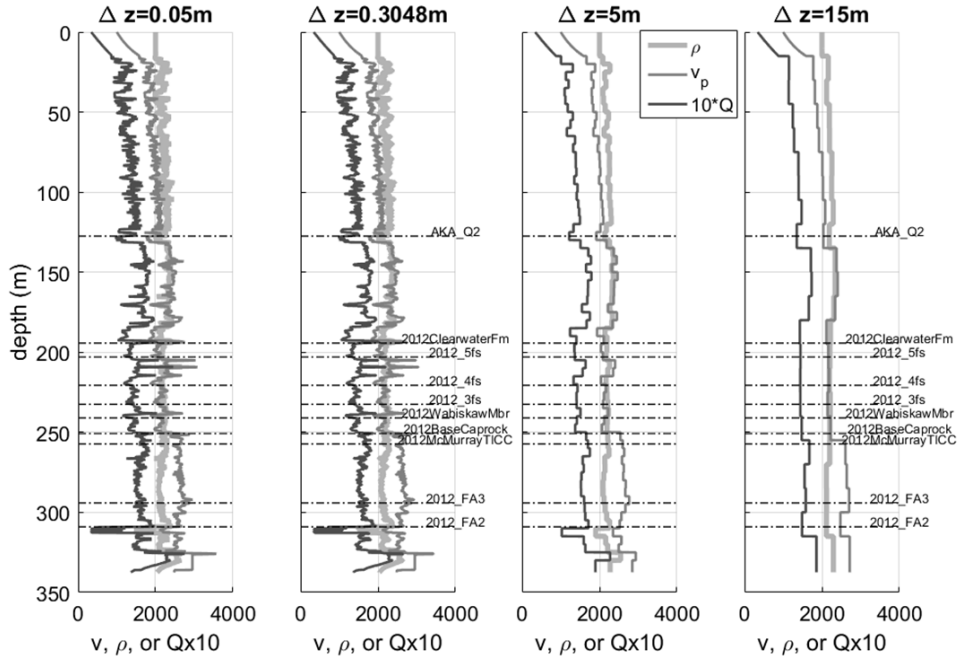

Figure 3: The logs of Figure 1 are shown after resampling with 4 different blocking sizes of 0.05m, 0.3048m, 5m, and 15m. The smallest block size is essentially the same as the original sample size while the others required averaging pf material parameters by the Backus method. For each block size and empirical Q model is also shown and was computed by the method of Margrave 2013. The upper 15m were not logged and are filled by a postulated overburden model.

1D synthetic VSP's for each of the four earth models are shown in Figures 4, 5, and 6. The computation algorithm creates the downgoing and upgoing fields separately and then sums them for the total field so, unlike real data, there is no separation error. Included in the computation are direct and reflected p-waves plus all possible multiples as defined by the reflectivity of the earth model. Also included are the effects of transmission loss, minimum phase Q attenuation, and frequency-dependent phase velocities. Significant effects that are not included are mode-conversion (to s-waves), offset dependent reflectivity, and wavefront spreading. The source was placed at $z = 0$ and emitted a 100Hz dominant minimum-phase wavelet.

A visual comparison of these VSP wavefields suggests that the results for blocking sizes of $\Delta z = 0.05$m and $\Delta z = 0.3048$m are very similar while the results for $\Delta z = 5.0$m and $\Delta z = 15$m are distinctly different. Figure 8 shows individual traces from each of the VSP wavefields corresponding to the deepest receiver. Also shown are first-break picks from the real VSP acquired in the same borehole and to be discussed shortly. These picks agree very well with all of the synthetics suggesting that the 15m overburden is at least consistent with the observed traveltimes. Inspection of these traces confirms the close similarity of the results for $\Delta z = 0.05$m and 0.3048m and it is noteworthy that the coda (the sequence of events after the first breaks) is much stronger for these traces than for the more strongly blocked results. The Fourier amplitude spectra of these four traces are shown in Figure 9. As the blocking size gets larger, the spectra become increasingly smooth. This can be understood by considering the spectral notching effect induced by two identical wavelets with a time separation t_0. Suppose we have the signal

$$s_1(t) = w(t) - w(t - t_0) = w(t) \cdot \big(1 - \delta(t - t_0)\big) \tag{1}$$

where $w(t)$ is a wavelet, $\cdot$ denotes convolution, and $\delta(t)$ is the Dirac delta function. Straight forward computation shows that the Fourier transform of s_1 is

$$\widehat{s_1}(f) = 2\widehat{w}(f)\sin(\pi t_0 f)\, e^{-i\pi t_0 f + i\pi/2}. \tag{2}$$

Similarly, the signal

$$s_2(t) = w(t) + w(t - t_0) = w(t) \cdot \big(1 + \delta(t - t_0)\big) \tag{3}$$

has Fourier transform

$$\widehat{s_2}(f) = 2\widehat{w}(f)\cos(\pi t_0 f)\, e^{-i\pi t_0 f}. \tag{4}$$

Comparison of equations 2 and 4 shows that a signal consisting of the sum of a wavelet and an identical delayed wavelet has an amplitude spectrum that is twice the wavelet's amplitude spectrum multiplied by a sine or cosine with argument $\pi t_0 f$. The sine occurs when the second wavelet has reversed polarity and the cosine occurs when the two wavelets have the same polarity. Thus $|\widehat{s_1}(f)|$ is essentially similar to $|\widehat{w}(f)|$ except for the introduction of spectral notches at the frequencies $f_n = {}^{n}/_{t_0}, n = 0,1,2\cdots$ which are the frequencies at which the sine function has zeros. Similarly, $|\widehat{s_2}(f)|$ has notches at the frequencies $f_m = {}^{m}/_{2t_0}, m = 1,3,5\cdots$. In both cases the sequence of notches has a spacing of t_0^{-1} but the essential difference is that $|\widehat{s_1}(f)|$ has a notch at 0Hz while $|\widehat{s_2}(f)|$ does not. This analysis is idealized but is suggestive of what happens in the case of a generalized sequence of internal multiples such as occurs here. A given multiple will appear as a copy of the original wavelet delayed in time and scaled by a reflection coefficient, R, which is a number between -1 and 1. Numerical experimentation shows that the effect of scaling the delayed wavelet by $|R| < 1$ is to reduce the depth and severity of the spectral notches. Figure 10 shows the results of a simple numerical experiment for 5 different values of R. The original wavelet is a 30 Hz Ricker whose spectrum can be seen as that for $R = 0$. Of course, a long sequence of interbed multiples is far more complex than this simple analysis; however, it is reasonable to infer that the occurrence of such multiples introduces notches into the spectrum, one for every pair of events, albeit at unpredictable frequencies. Since the notch frequencies are inversely proportional to the separation, it follows that many closely spaced multiples will produce many notches at higher frequencies. The result is the stratigraphic filtering effect predicted by O'Doherty and Anstey (1971).

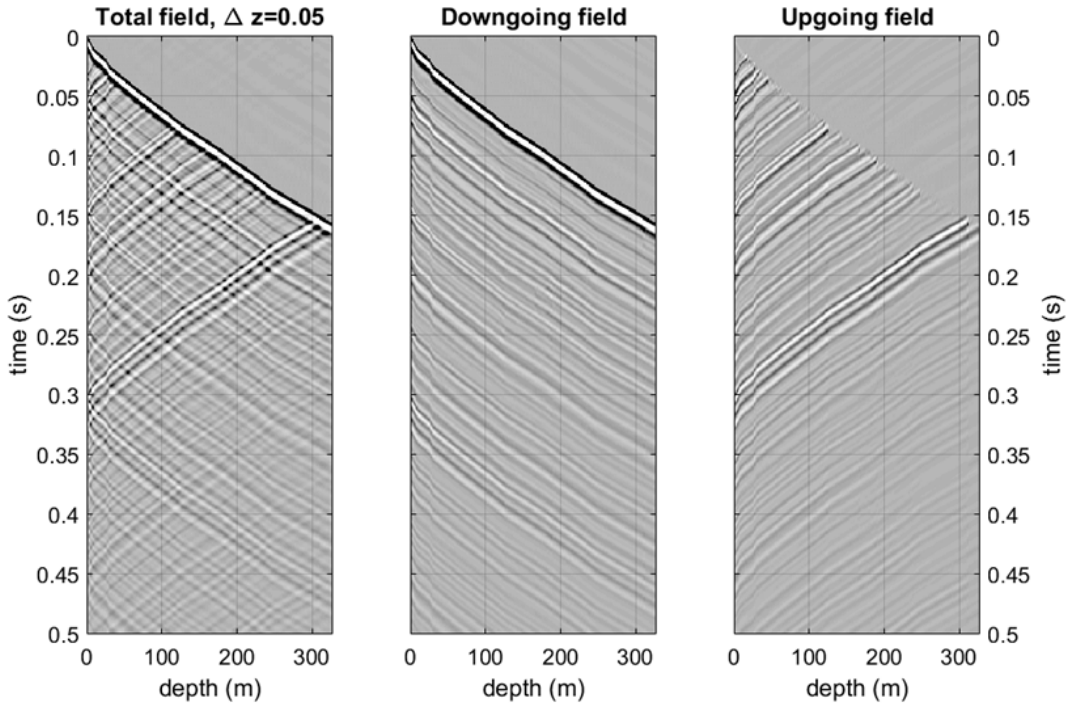

Figure 4: The 2D synthetic VSP for a surface source computed according to Margrave (2014b) for the model of Figure 3 having a blocking size of $\Delta z = 0.05$m. The total field (left) is the simple sum of the downgoing field (middle) and the upgoing field (right). The downgoing and upgoing fields are computed separately and then summed for the total field so there is no separation error.

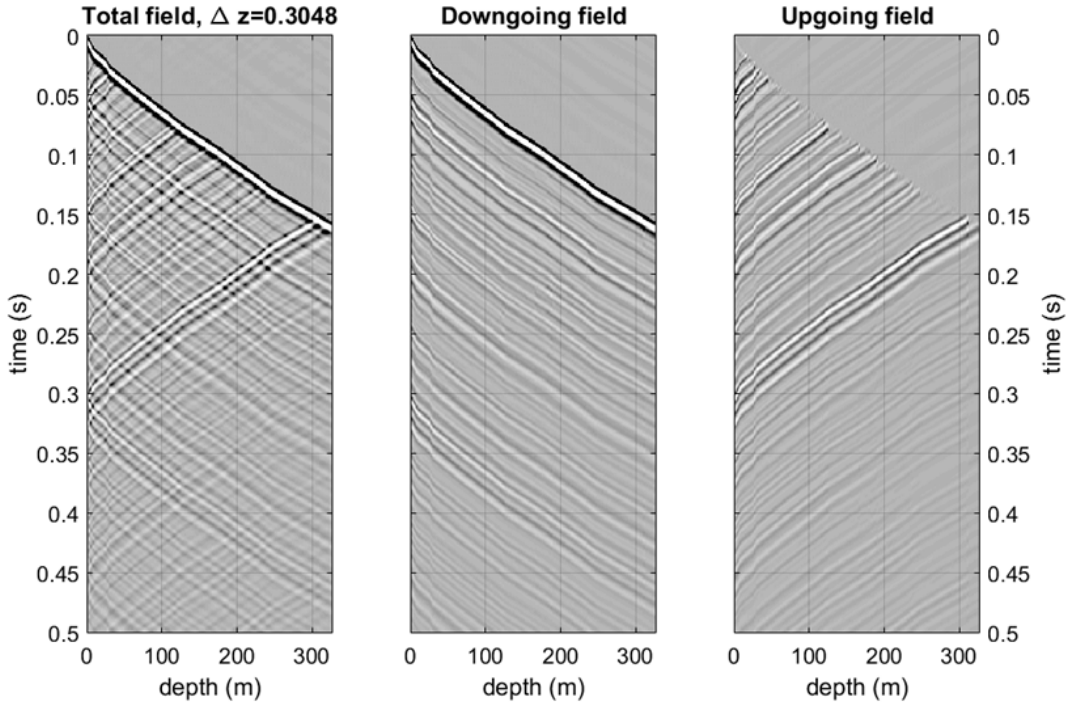

Figure 5: Similar to Figure 4 except that the earth model has the blocking size of $\Delta z = 0.3048$m and is shown second from left in Figure 3.

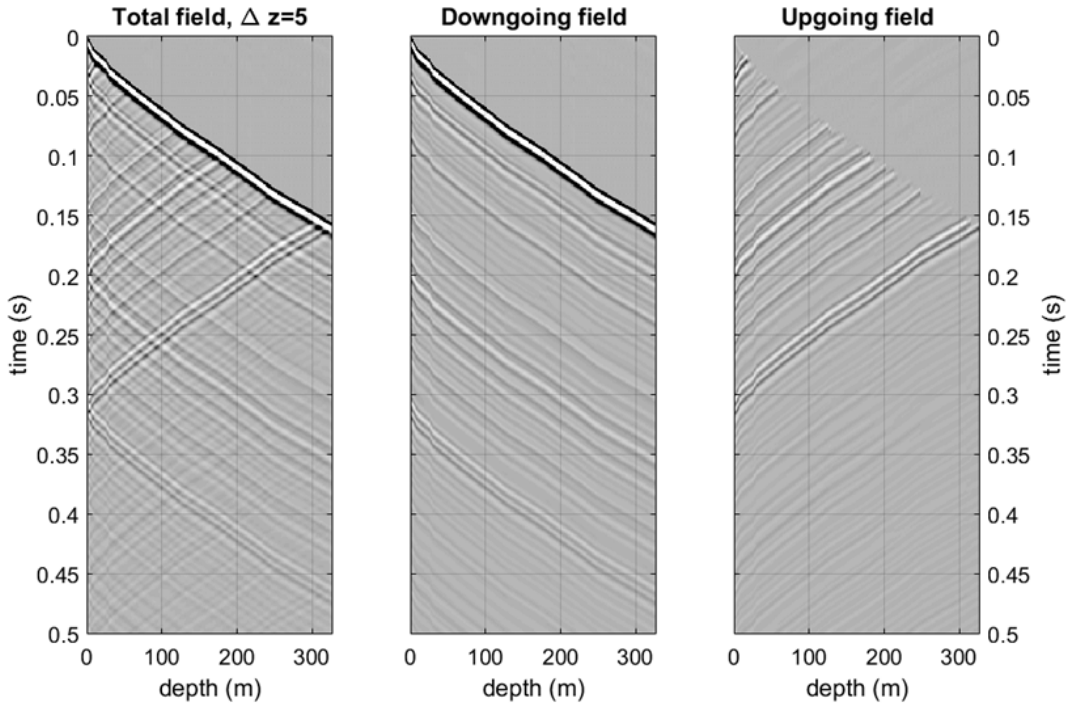

Figure 6: Similar to Figure 4 except that the earth model has the blocking size of $\Delta z = 5.0$m and is shown third from left in Figure 3.

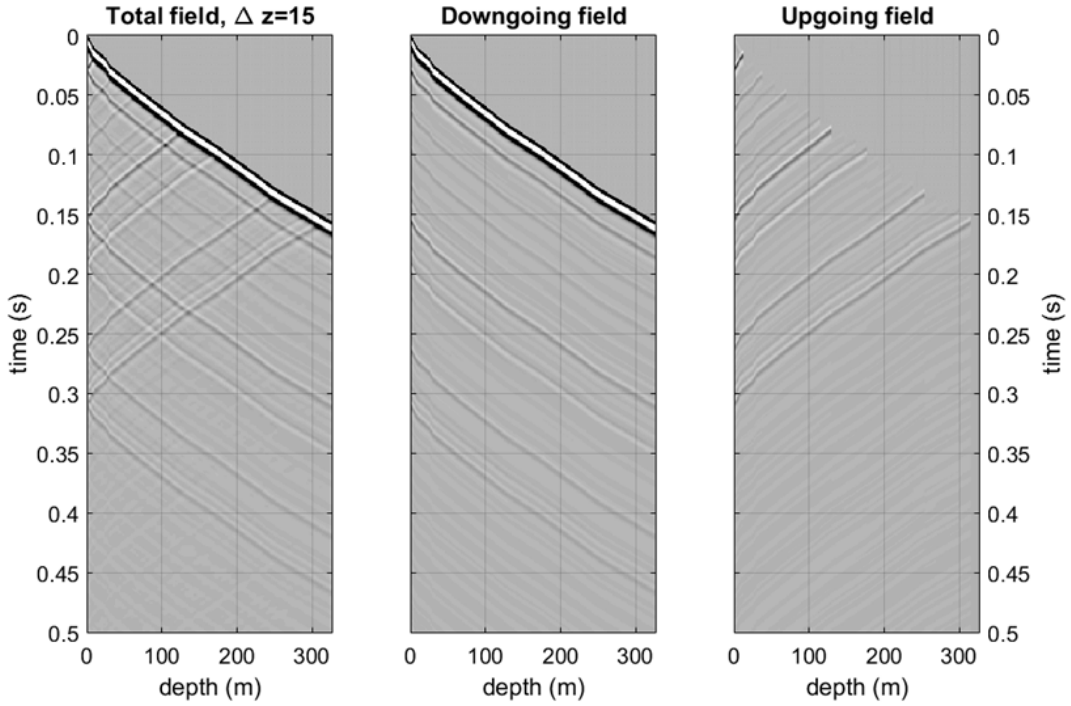

Figure 7: Similar to Figure 4 except that the earth model has the blocking size of $\Delta z = 15.0$m and is shown on the far right in Figure 3.

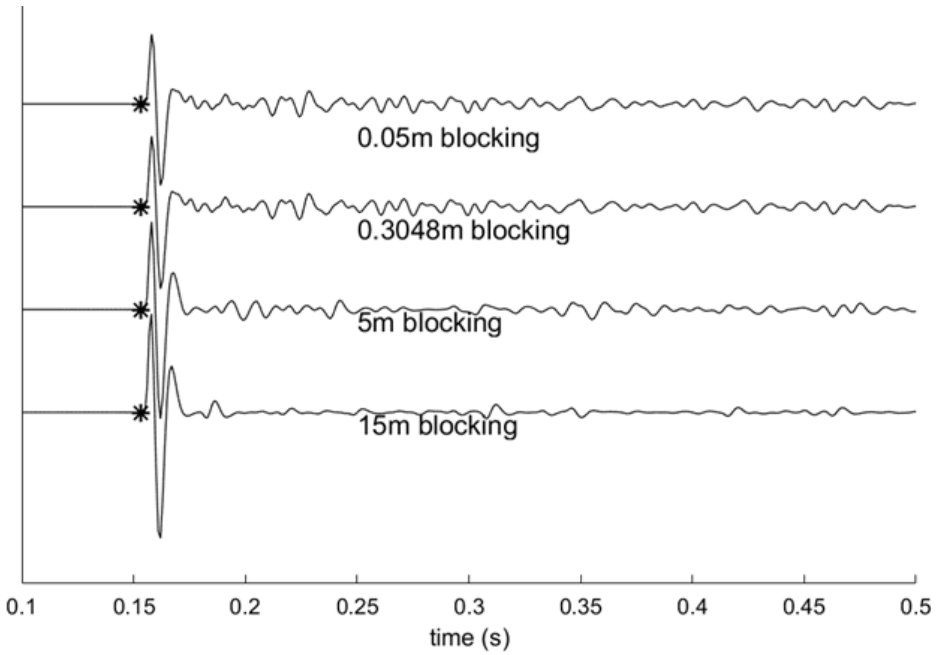

Figure 8: Single traces from each of the wavefields for the previous 4 figures corresponding to the deepest receiver and the total field. The asterisk on each trace is placed at the measured first break time of the real VSP shot in this same well.

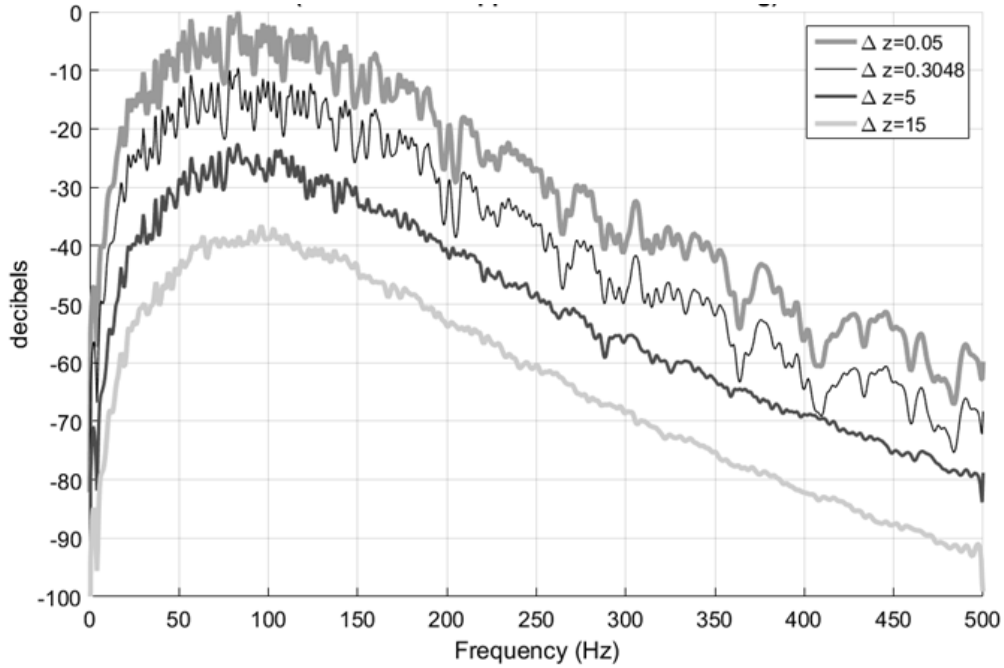

Figure 9: The Fourier amplitude spectra of the four traces in Figure 8. A vertical shift has been applied to avoid over plotting as each spectrum has nearly the same maximum. As the blocking size (Δz) increases, the spectra become increasingly smooth.

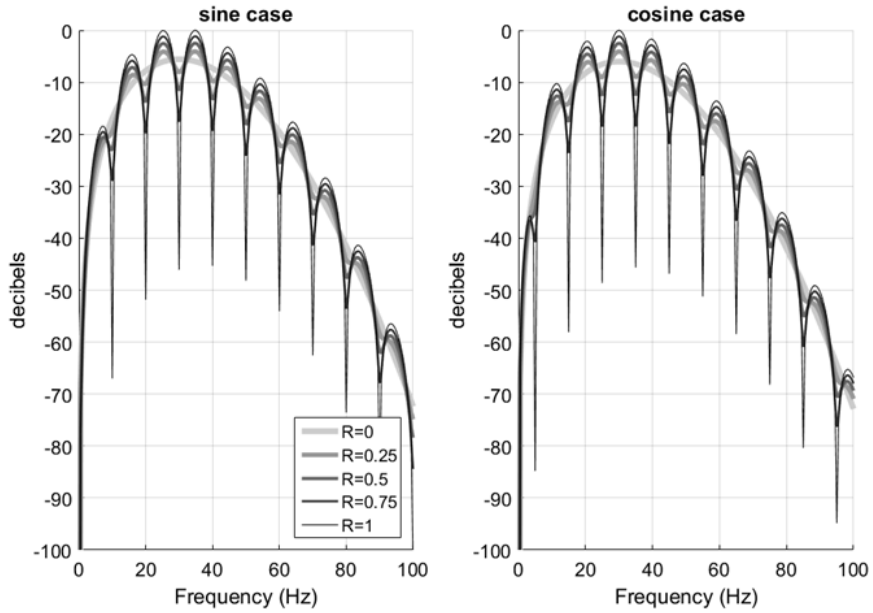

Figure 10: The results of a numerical experiment based on modifications of equations 1 and 3. One the left are the Fourier amplitude spectra of 5 different signals of the form $w(t) - Rw(t - t_0)$ where $w(t)$ is a Ricker wavelet, $t_0 = 0.1$s, and $= 0, 0.25, 0.5, 0.75, 1.0$. On the right is a similar experiment for the signal $w(t) + Rw(t - t_0)$. Note the positions of the spectral notches and that the notch depth depends upon R.

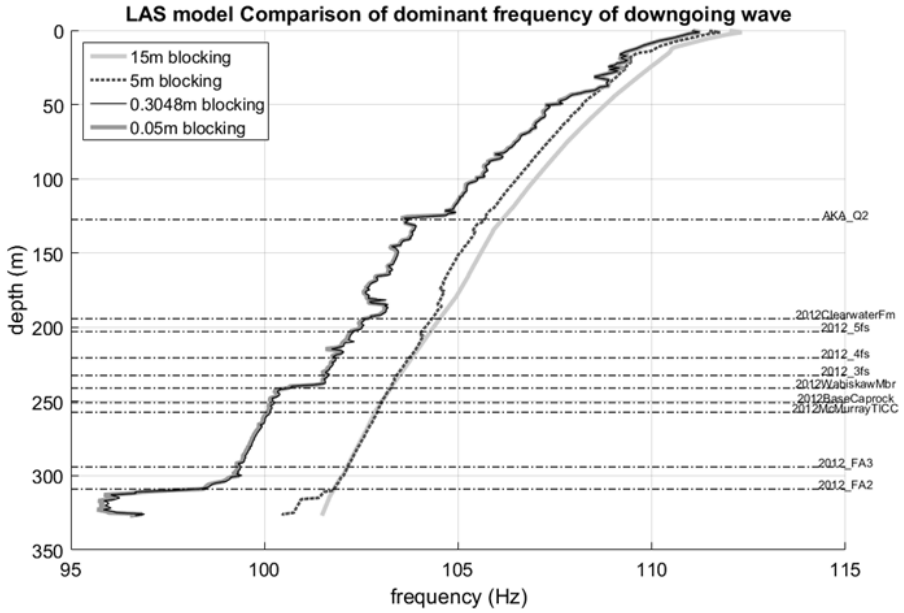

Figure 11: The decay of dominant frequency with depth is shown for each of the four downgoing wavefields of figures 4, 5, 6 and 7. Blocking sizes of $\Delta z = 0.05$m and $\Delta z = 0.3048$m give essentially identical results while the other two are very different. The curve for 15m blocking has virtually no stratigraphic filtering and is therefore showing only intrinsic Q. The difference between this curve and the others is due to stratigraphic filtering.

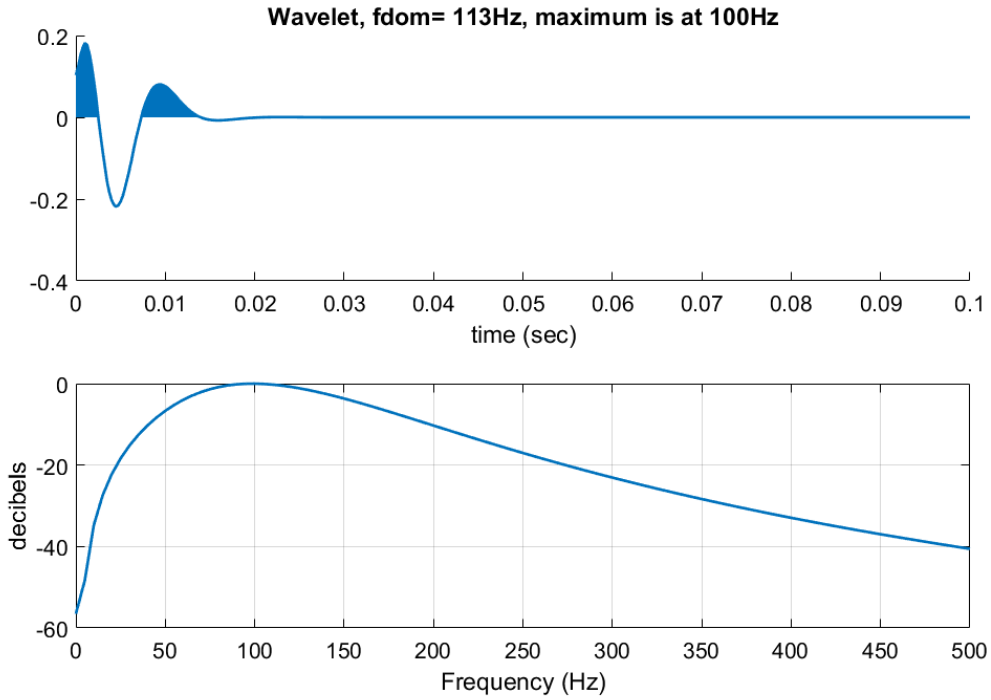

Figure 12: The wavelet used in the simulations of Figures 4-7 and its amplitude spectrum. The amplitude spectrum has a maximum at 100Hz but its dominant frequency as computed by equation 5 is 113Hz.

Margrave (2014a, see also Figure 2 of this paper) showed that the Q-like effects of stratigraphic filtering, as predicted by O'Doherty and Anstey (1971), are essentially nil for blocking sizes greater than about 10m when other parameters (e.g. log length) are similar to those used here. A direct indicator of total attenuation (intrinsic plus stratigraphic) is the decay of dominant frequency with propagation distance. In fact, this can be used to measure the Q value as will be shown. Figure 11 shows the decay dominant frequency with depth for the downgoing wavefields of the four experiments in Figures 4, 5, 6, and 7. Here dominant frequency is calculated by

$$f_{dom} = \frac{\sum_k f_k A_k^2}{\sum_k A_k^2} \tag{5}$$

and is sometimes called the centroid or power-centroid frequency. In this equation, the sum extends over all non-negative frequencies, f_k is the frequency of the k^{th} sample, and A_k is the amplitude spectrum of the k^{th} sample. Defined in this way, the dominant frequency is influenced by the shape of the amplitude spectrum and is not simply the frequency where the spectrum is maximal. This is especially valuable for spectra like those in Figure 9 which have a complex structure. Figure 12 shows the wavelet used in these simulations for which equation 5 gives $f_{dom} = 113$Hz whereas the amplitude spectral maximum occurs at 100Hz. Inspection of Figure 11 shows that the measured dominant frequency begins just below 113Hz at $z = 0$ and then decays strongly with depth. The decay curve for $\Delta z = 15$m has almost no stratigraphic component and decays essentially monotonically. This is to be expected for intrinsic attenuation which suffers amplitude spectral decay according to $e^{-\pi f t/Q}$ where Q is the intrinsic Q factor meaning

that which is directly due to viscoelastic behaviour of rocks. On the other hand, the stratigraphic attenuation of O'Doherty and Anstey is a result of the superposition of very many interbed multiples each with their own unique delay. The resulting spectral decay is caused by destructive interference, has nothing to do with viscoelasticity, and will be observed even for a perfectly elastic medium. Put another way, intrinsic attenuation represents transference of energy from the seismic wave to the rock matrix where it manifests as heat. Stratigraphic attenuation does not indicate energy transference but rather energy delay. Given sufficient recording time and accuracy, the propagating seismic wave would be found to have no energy loss due to stratigraphic attenuation. The stratigraphic interference effect is essentially a statistical argument and there is no requirement of monotonic decay. Instead, there is a steady decay but there are ups and downs as can be seen in the decay curves for $\Delta z = 0.05$m or 0.3048m. We conclude from this figure that either of the two finest blocking sizes are sufficient to estimate the stratigraphic effect as there is very little difference in their dominant frequency decay curves.

The dominant frequency can be considered to be an attenuation attribute but is not actually attenuation. For a more direct measurement we can choose either to estimate Q or its inverse. Here we examine *cumulative attenuation* as defined by Hauge (1981) and computed by

$$CA = \frac{\pi(t_2 - t_1)}{Q_{1,2}} \tag{6}$$

where t_1 and t_2 are the arrival times (first-break times) of the VSP downgoing wave at receivers 1 and 2, and Q_{1-2} is the estimated effective Q value between these receivers. The Q value can be difficult to measure and is especially error prone when the attenuation is small and noise is present. In this case Q tends to be a large number with a large error; however, CA is small with a small error. So, while the computation of CA requires first an estimation of Q, the subsequent calculation of CA tends to de-emphasize the most problematic Q estimates.

In the present case, consider the measurement of Q and CA on the downgoing wavefield for the synthetic VSP computed with $\Delta z = 0.05$m (Figure 4). Let the receiver at 66.4m depth be taken as a reference (this choice seems arbitrary but is made for comparison with our real VSP which will be shortly discussed). Then for each receiver beneath this reference we estimate Q and CA by comparing the traces at each receiver to the trace at the reference receiver. For each estimation, we will refer to the second receiver as the analysis level. A 0.2s time window is selected beginning at the first break for both levels and Q is estimated by the spectral ratio method and by the dominant frequency method (Margrave, 2013, describes the methods and the software). This means that our measures are average values for the interval between the two receivers. Figure 13 compares Q and CA measures for the two different calculation methods and demonstrates issues discussed in the previous paragraph.

The spectral ratio method is widely used and requires the *log-spectral ratio*, or lsr, to estimate Q. The *lsr* is formed by first computing the Fourier amplitude spectrum at the reference level, A_1, and again at the analysis level, A_2. The lsr is then formed as $lsr =$

$\ln(A_2/A_1)$. From constant Q theory, it then follows that the lsr should be a linear function of frequency ($lsr = -\pi f(t_2 - t_1)/Q_{1,2}$) and that Q can be estimated from the slope of a least-squares fit of a straight line to the lsr. While seemingly simple, the spectral-ratio method is weakened by its dependence on the division of two independent measurements which will be problematic for noisy data. Experience shows that the expected linear-with-frequency behaviour of the lsr will only be observed over a limited frequency range and this range can be difficult to predict. Moreover, the Q estimate is inversely proportional to the slope of the lsr. This means that, for low attenuation, the slope will be small and Q will be large. Small errors in slope will cause large errors in Q.

The dominant-frequency method is a nice contrast to the spectral-ratio method in that it is independent of the frequency band and does not require a division so it is less sensitive to noise. The method assumes a Q value and uses it to estimate the attenuation of spectrum A_1 after propagation to level 2 as $A_{1Q} = A_1 e^{-\pi(t_2 - t_1)/Q}$. The estimated Q will be that for which the dominant frequency of A_{1Q} comes closest to that measured from spectrum A_2. This can be found by a direct search that tests all integer Q values in an assumed range (here $5 \leq Q \leq 500$). The dominant-frequency method is far less sensitive to noise than the spectral-ratio approach and it is also insensitive to amplitude balancing issues that might occur in acquisition or processing.

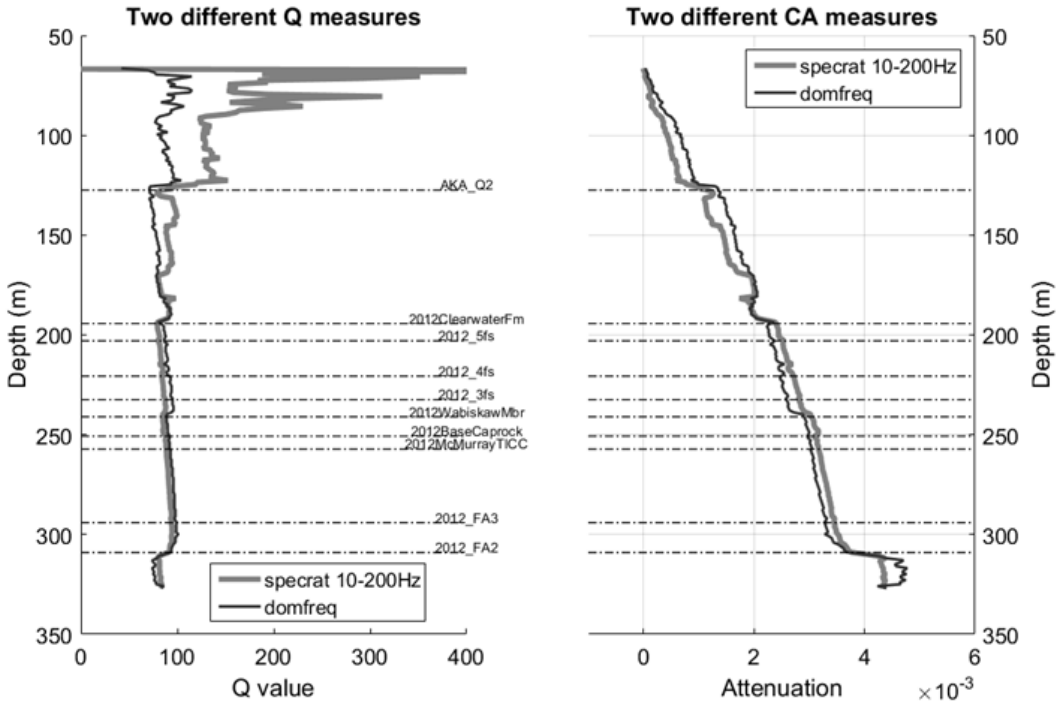

Figure 12: Two different Q measures and the corresponding CA measures are compared for the downgoing VSP field of Figure 4. The receiver at z=66.4m was designated as a reference and then the wavefield at each deeper receiver was compared to the reference to estimate the average Q for the interval between receivers. CA was then calculated by equation 6. The results are plotted versus the depth of the second receiver. The spectral ratio estimates were performed over the 10-200 Hz band.

Figure 12 shows that the two methods give significantly different Q estimates even on a noise-free synthetic. It is not easy to say which one is correct because we are measuring an effective attenuation including both intrinsic and stratigraphic effects. The former is known but the latter is not. Above 130m, attenuation is slight and the spectral-ratio method gives large Q values with large fluctuations. For analysis depths greater than 130 m the methods give more comparable Q estimates. Alternatively, the CA estimates, while being slightly different everywhere are consistent in trend and overall shape. Changing the frequency band for the spectral-ratio estimates will always give different results. The band chosen here was selected after some experimentation because it gave results that were the most consistent with the dominant-frequency method.

Stratigraphic Q and intrinsic Q combine to give the effective Q, which is what can be directly measured, according to (Richards and Menke, 1983)

$$Q_{eff}^{-1} = Q_{intrinsic}^{-1} + Q_{strat}^{-1}. \tag{7}$$

The equivalent relation for CA measures is

$$CA_{total} = CA_{intrinsic} + CA_{strat} \tag{8}$$

Having measured CA_{total} and knowing $CA_{intrinsic}$ (see figure 2) we can now estimate CA_{strat}. Figure 13 shows this estimation for the spectral-ratio method and Figure 14 does the same for the dominant-frequency method. Of note in both figures is that intrinsic attenuation is monotonically increasing while total and stratigraphic attenuation are not monotonic although they generally increase. When computed with respect to a fixed reference level as we have done, intrinsic attenuation should never decrease as the analysis depth (the depth being compared to the reference depth) increases. This is because the $CA_{intrinsic}$ for a particular receiver is just the value estimated for the receiver just above it plus a value for the local attenuation between receivers. (Intrinsic attenuation is the same in both figures as it is prescribed in the model.) Also, the sudden fluctuations in both CA_{strat} and CA_{total} are due to stratigraphic effects. Figure 15 compares the two estimates of CA_{strat} where it becomes obvious that the spectral-ratio method measured essentially no stratigraphic effect for the interval about 130m. While there was measured attenuation, it followed very closely to the intrinsic trend. On the other hand, the dominant-frequency method suggests that there is significant stratigraphic attenuation in this interval. This point needs further investigation. Nevertheless, the two estimates are reasonably close and suggest that CA_{strat} is a significant effect representing, in this case, 40-50% of the total attenuation.

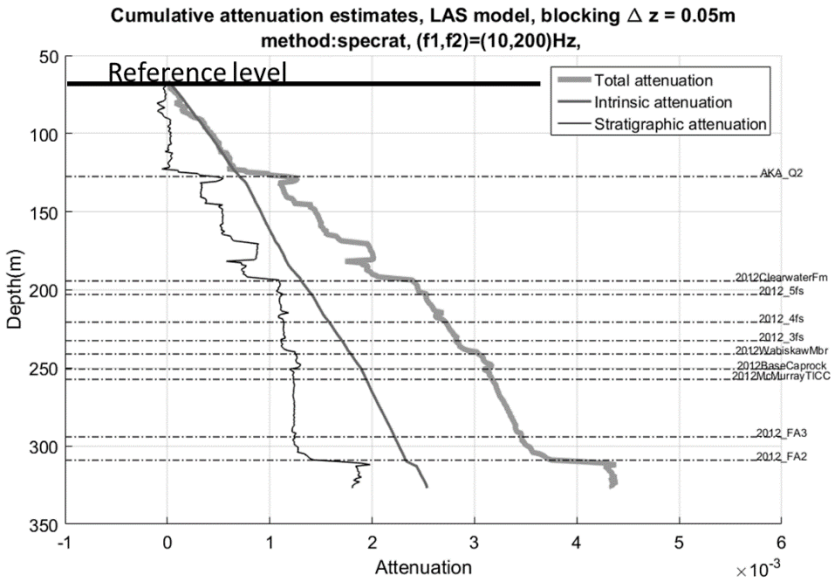

Figure 13: The estimate of stratigraphic attenuation by the spectral ratio method.

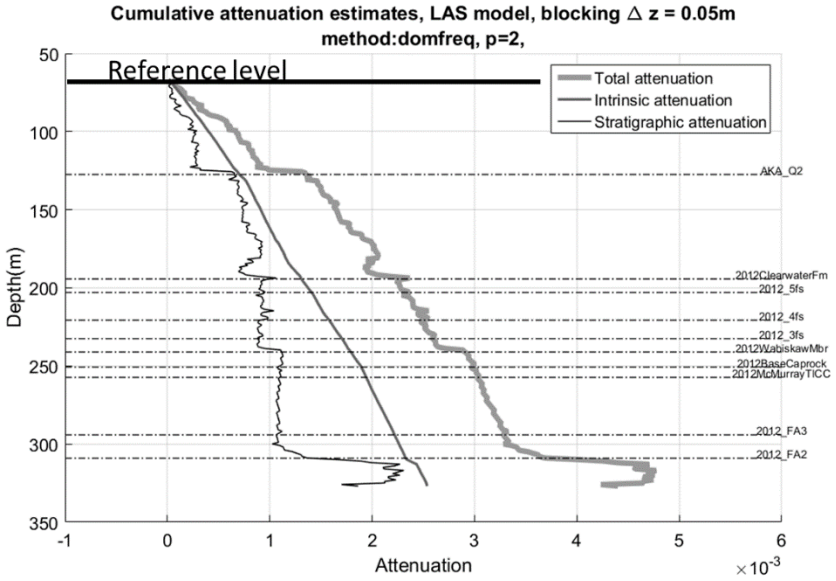

Figure 14: The estimate of stratigraphic attenuation by the dominant frequency method.

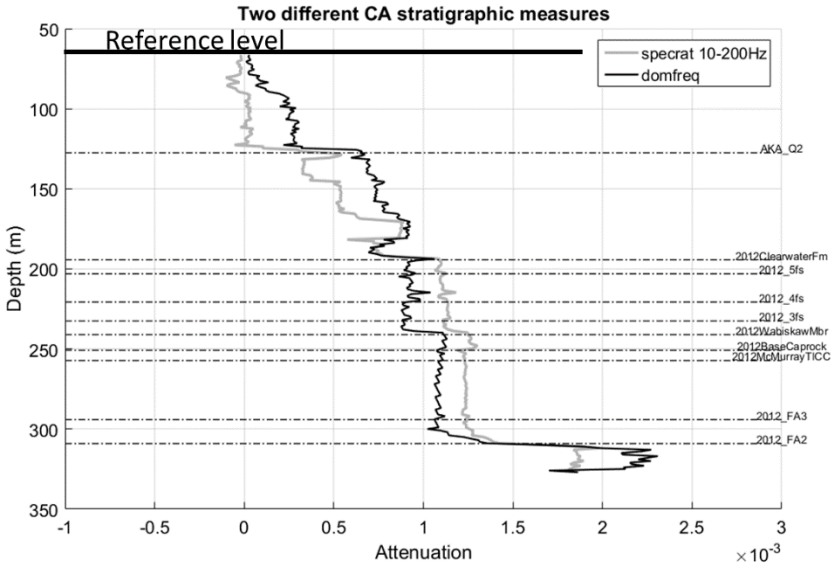

Figure 15: Comparison of the stratigraphic attenuation estimates from figures 13 and 14. The light gray curve is estimated by the spectral-ratio method while the black curve is estimated by the dominant frequency method.

STRATIGRAPHIC CORRECTIONS APPLIED TO REAL VSP ATTENUATION

A VSP was acquired in the same borehole as the well logs used previously to create the synthetic VSP's of Figures 4-7. The receiver configuration used a special tool that allowed placement of single 3C geophones roughly every meter beginning just beneath the Kelly bushing. Figure 16 compares the real VSP with the synthetic of Figure 4. Both have exactly the same receiver positions and the real VSP has t^2 gain applied but no other processing. Immediately apparent is the low frequency noise contaminating the shallow receivers on the real VSP. While there are similarities in the pattern of reflected waves in both, there are differences too. The missing upper 15m of the well logs (see figures 1 and 3) has some bearing on this; but of greater effect is that the sonic log was synthetized from the density log for depths above 150m which gives an incorrect reflectivity. Also, it appears that the real data has higher frequency content than the synthetic. The wavelet used in the synthetic was chosen be minimum phase and to have a dominant frequency of 113 Hz which was similar to the real data. However, Figure 17 confirms that the synthetic has a slightly lower amplitude spectrum at both the very high and very low frequencies. Recalling that the source for the real VSP was a dynamite charge, we see that our wavelet is an imperfect model for this source. This should not be of concern because the estimate of attenuation is about the decay of frequency content with propagation, meaning that it is the relative frequency loss between any two receivers and not the absolute spectral amplitudes that matters here.

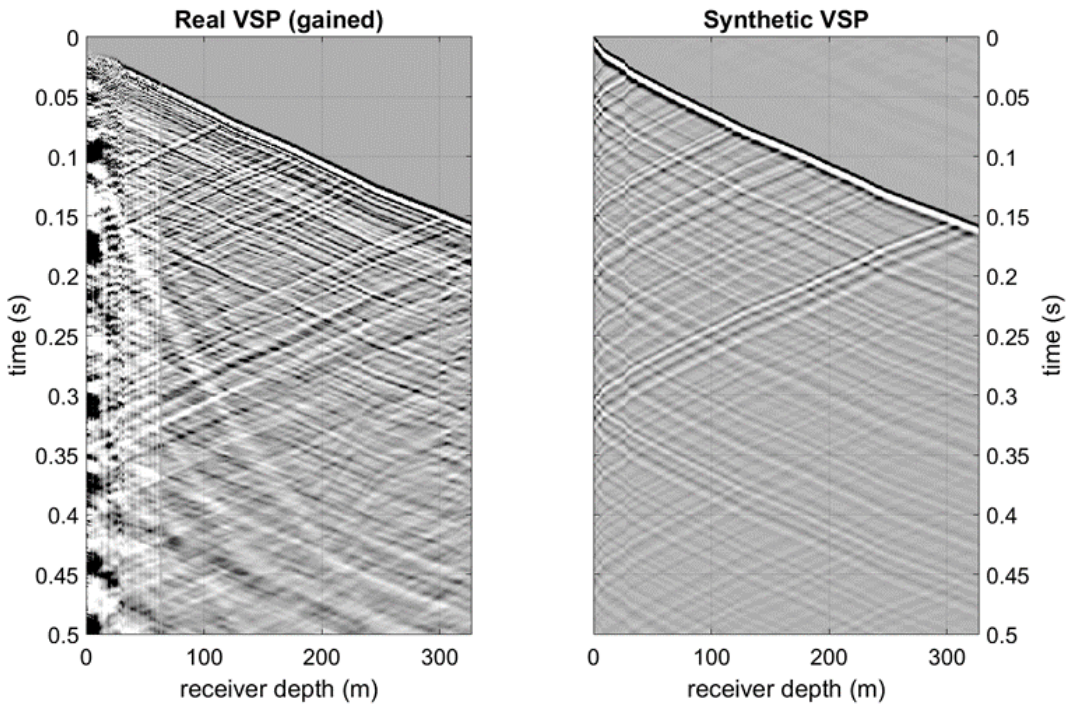

Figure 16: Comparison between the real VSP (after t^2 gain) and the synthetic VSP of Figure 4.

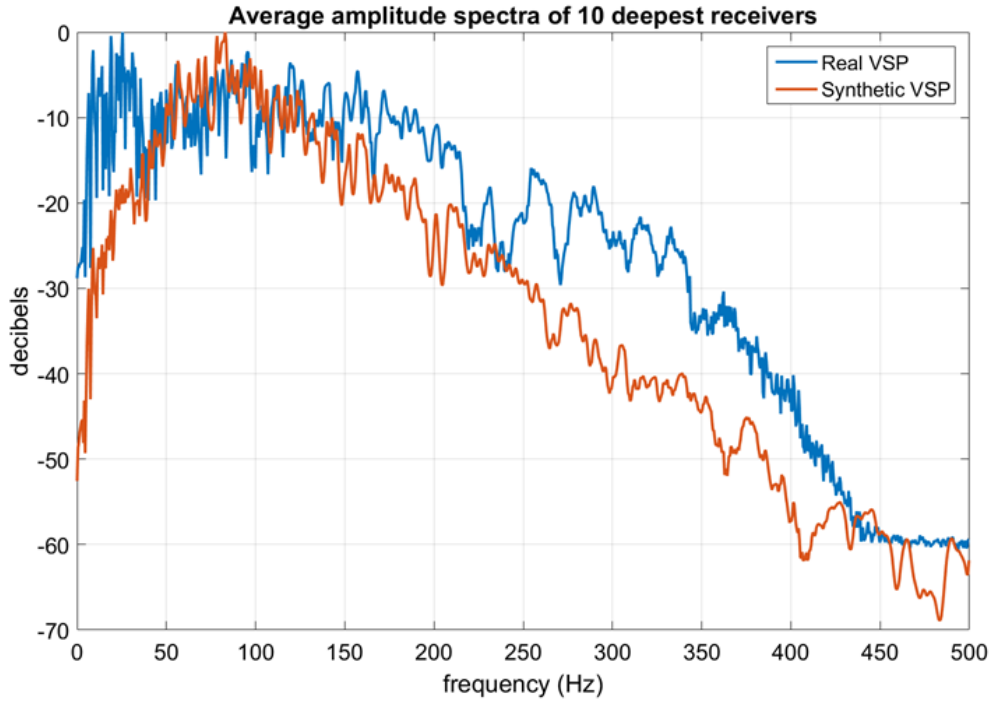

Figure 17: The average amplitude spectra of the 10 deepest receivers for the two VSP wavefields shown in the previous figure. It is apparent that, while similar in dominant frequency, the real VSP has a more broadband spectrum.

The measurement of CA requires a separated downgoing field. This was done by a third-party contractor with the result shown in Figure 18 and compared to the synthetic

downgoing field. It is apparent that these two fields are quite different. Among the most obvious differences are low-frequency artefacts contaminating the shallow receivers and the overall amplitude decay due to wavefront spreading. The latter is of little concern as frequency-dependent attenuation estimates are easily separated from frequency-independent amplitude loss. However, the former is a significant complication and, as will be seen, introduced effects that are outside the current theory. This low-frequency noise is very likely due to receiver coupling problems in the upper portion of the borehole. In an attempt to avoid the worst effects of this noise, a reference depth for our CA computations was chosen at 66.4m depth which is below the largest disturbance.

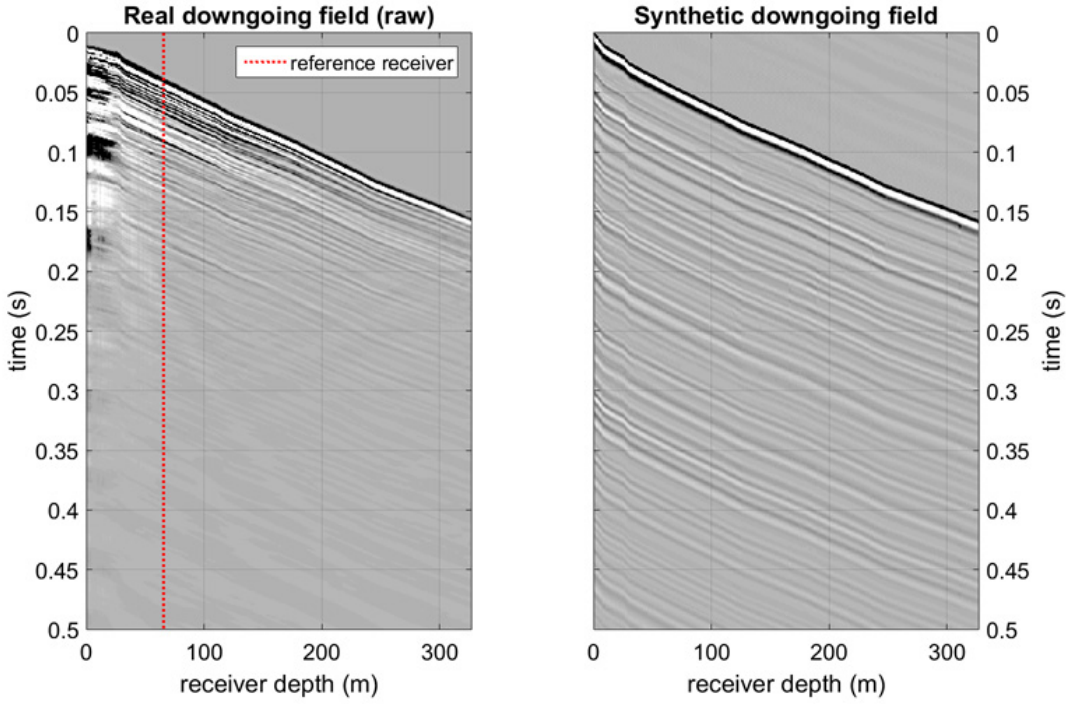

Figure 18: The downgoing field as estimated by a third-part contractor (left) is compared to the synthetic downgoing field created from well logs.

Figure 19 shows an attempt to correct total attenuation measures using the stratigraphic estimates shown in Figure 15. The third-party contractor provided an estimate of total CA using a proprietary algorithm and we computed another estimate using the dominant-frequency method. Both estimates were then corrected for stratigraphy using equation 8 solved for $CA_{intrinsic}$. The two estimates of total attenuation differ dramatically for depths above 190m but become quite close below this level. The results for intrinsic attenuation are far from satisfying and show many obvious problems. Perhaps the most significant is that the estimate of $CA_{intrinsic}$ is not a monotonically increasing function as theory expects (see Figure 14). Since the measured CA_{total} shows many rapid increases and decreases, a compatible CA_{strat} must remove these by subtraction to produce a monotonically smooth intrinsic estimate.

In order to reduce the effects of the artificial sonic log above 150m we consider the estimation of CA relative to a deeper level and choose the top of the formation '2012ClearwaterFM' (194m depth) as the new reference. Let $z_1 < z_2 < z_3$ be three

receiver depths, then denote by $CA_{1,3}$ the attenuation at level 3 relative to level 1 and by $CA_{2,3}$ the attenuation at level 3 relative to level 2. Then it follows from the definition of CA and the form of the exponential Q attenuation, that

$$CA_{1,3} = CA_{1,2} + CA_{2,3}, \tag{9}$$

or

$$CA_{2,3} = CA_{1,3} - CA_{1,2}. \tag{10}$$

Thus to adjust CA to a deeper level, we simply subtract the CA for the interval between the old and new reference levels. Figure 20 shows the new estimates and simply amounts to a change of origin for the lower portion of Figure 19. While we are now able to focus on the interval where the two estimation methods (that of the contractor and the dominant frequency method) give very similar answers, we still see the same problems as before with the intrinsic estimates. For example the strong decrease of intrinsic attenuation between 235m and 255m is not explicable as an intrinsic effect. This suggests that either our estimates of total attenuation are seriously in error or that our estimate of the stratigraphic effect is too small. The former seems unlikely since we have good agreement between two very different methods conducted by different researchers. More likely is that our estimation of the stratigraphic effect is too small and this may, in part, be due to our visco-acoustic assumption and the consequent neglect of mode conversions in the internal multiples.

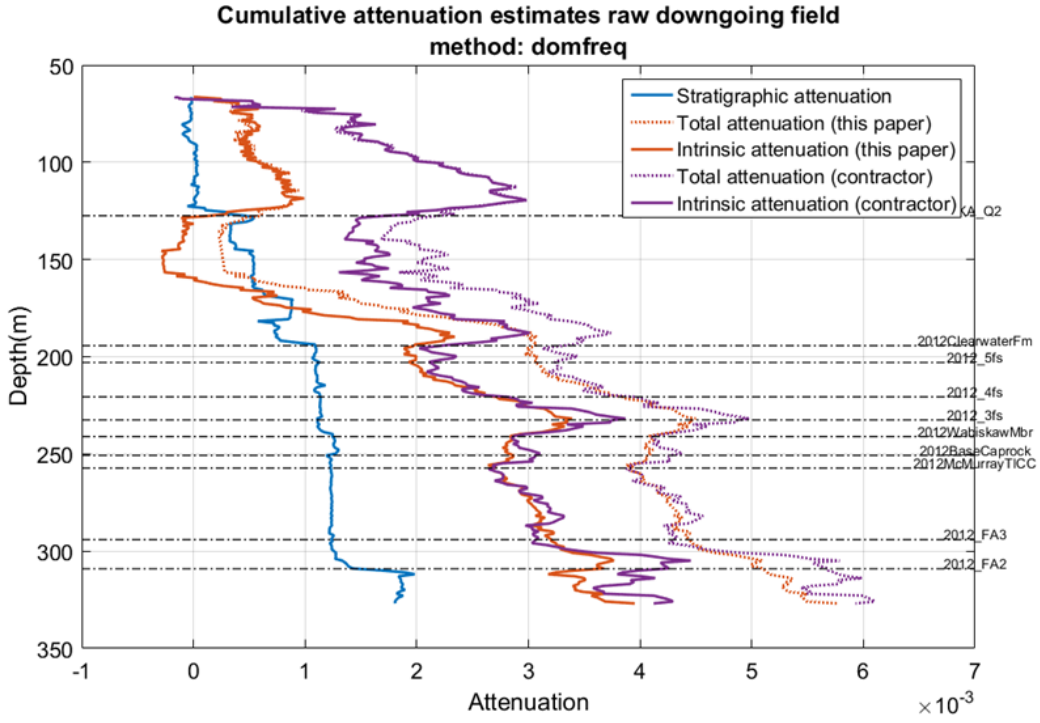

Figure 19: The application of the estimated stratigraphic attenuation to measured total attenuation. Two alternate estimates of total attenuation are shown as dotted lines. Both were calculated on the downgoing field of Figure 17, one by the contractor (purple) and the other by us

(orange). The solid orange and purple lines are estimates of intrinsic attenuation formed by subtracting the estimated stratigraphic attenuation from the corresponding estimate of total attenuation.

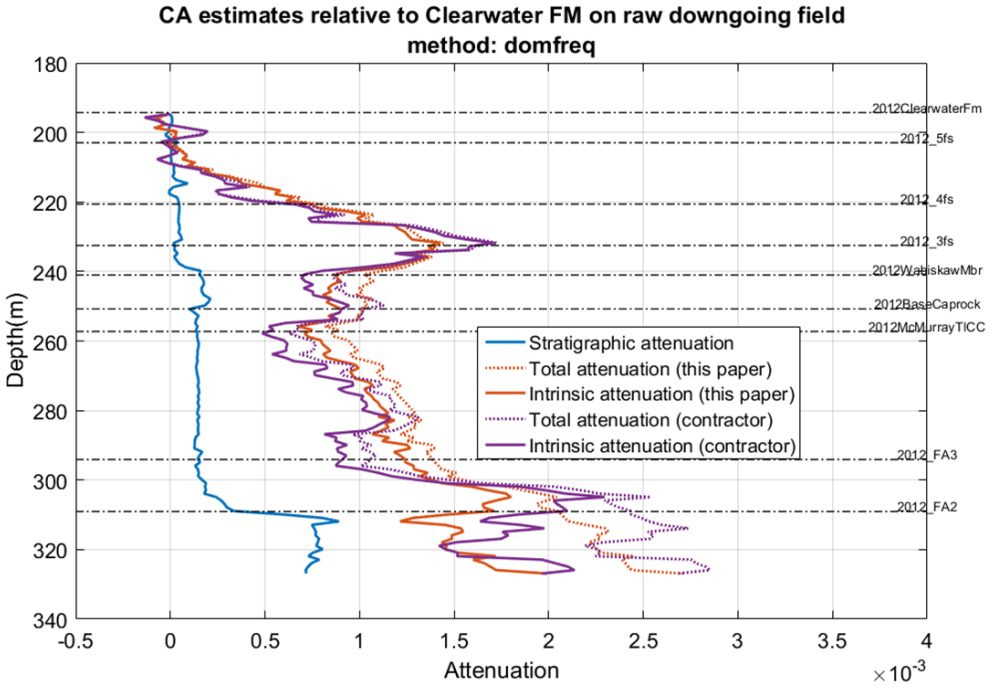

Figure 20: Similar to Figure 19 except that cumulative attenuation estimates are computed relative to the formation top '2012ClearwaterFm' which is at a depth of 194m.

Investigating further, Figure 21 shows the dominant frequency estimates for each receiver in both the real and the synthetic downgoing fields of Figure 18. The systematic decay of the estimate on the synthetic wavefield suggests what we would hope to see in the real data. Instead, the real data show a contorted pattern of dominant frequency that actually increases from 0 to the first reference depth (65.44m), decreases from there to about 120m where it again increases until 150m. From 150m to the end of the VSP at just less than 340m we see an overall decrease but there is another increase in the interval 230m-255m. The marked increase from 0 to 65.44m can be attributed to the influence of the low-frequency noise mentioned previously and attributed to receiver coupling problems. Ignoring the behaviour of this attribute for depths above 150m, from 150m to 340 the rather regular decay trend is interrupted by one interval of increase (230-255m) which is preceded by a similar interval (210-230m) of more rapid decrease. Possibly, this is a stratigraphic effect (both the rapid decrease and the increase) that is not accounted for by our 1D visco-acoustic analysis. It seems entirely possible that a visco-elastic effect, possibly associated with low rigidity could account for this but investigating that conjecture is beyond our current scope.

A further difficulty is the missing upper 15m of the well logs and the artificial nature of the sonic log used above 150m. Stratigraphic attenuation is a cumulative process that, at a given analysis depth, depends upon the stratigraphy of the entire overburden. The problems with our log above 150m could well affect our results far below this depth. This is a topic for further investigation.

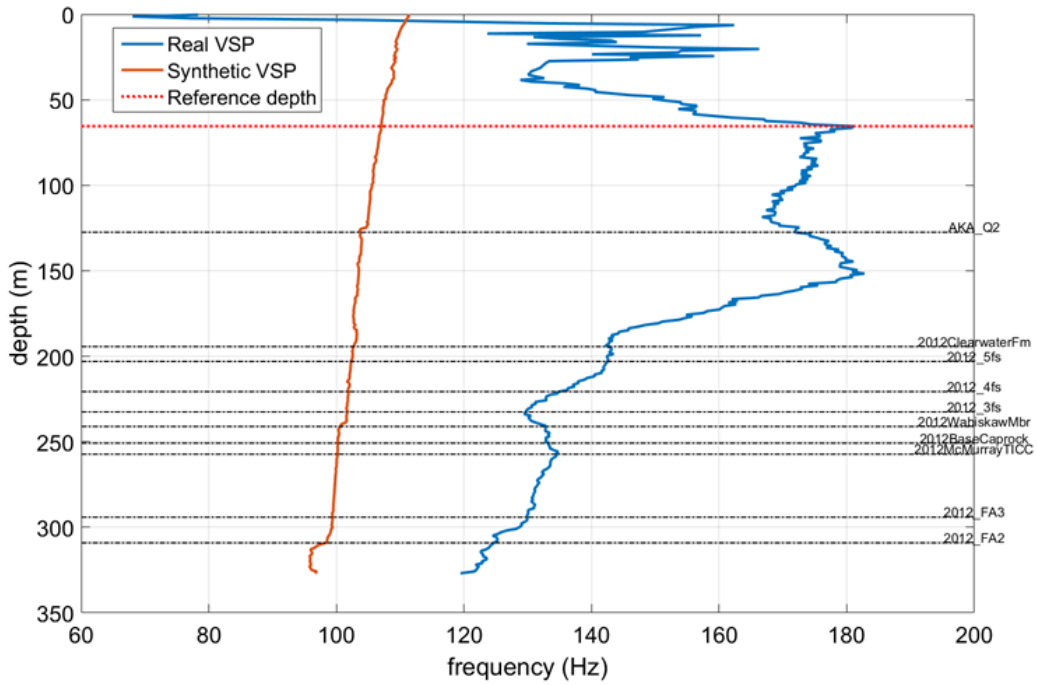

Figure 21: Estimates of dominant frequency for the two downgoing wavefields of Figure 17. The estimates were made for each receiver in a 0.5s window beginning at the first break times.

CONCLUSIONS

We have presented a study of stratigraphic filtering in a practical setting where both finely sampled well logs and a finely sampled VSP are available. The well logs were well sampled but the upper 15m was unlogged and the sonic log values above 150m were synthesised from the density log. Using the well logs we simulated a 1D VSP response that includes both intrinsic and stratigraphic attenuation. By measuring the total attenuation and with knowledge of the intrinsic attenuation, we then made estimates of the stratigraphic attenuation for four different earth models. The four models were created by blocking the logs at four different values: 0.05m, 0.3048m, 5m, and 15m. The acquisition sample interval was 0.3048m and the 0.05m sample size was achieved by interpolation. The last two sample sizes represent coarser blockings used to show that the stratigraphic effect disappears rapidly with loss of stratigraphic detail. We showed that the first two blocking values give a strong, essentially identical, stratigraphic effect which diminishes and vanishes by the final value. The measurement of attenuation is done on the VSP downgoing field and is therefore susceptible to errors in wavefield separation. Our synthetic VSP was created with perfectly separated downgoing and upgoing fields and does not have this problem. Wavefield separation of the real VSP was accomplished by a third party contractor and was complicated by low-frequency noise possibly related to poor receiver coupling in the upper part of the borehole and/or borehole waves. The contractor also provided measurements of total cumulative attenuation. Our attempts to correct these measurements for the stratigraphic effect, thereby estimating intrinsic attenuation, have been interesting but not fully satisfactory. Intrinsic attenuation, as a cumulative effect from a given reference level, should be a monotonically increasing function but our estimates do not conform to this expectation. It appears that our

stratigraphic attenuation estimate is too small to remove observed fluctuations in total attenuation. Perhaps the mostly likely cause for this is our neglect of the possibility of mode conversions in the internal multiple chain. It seems very likely that inclusion of this elastic-wave effect will increase the overall stratigraphic attenuation. Other difficult issues are the difficulties with wavefield separation, the unlogged upper 15m, and the artificial nature of our sonic log above 150m. A future field experiment would be recommended to include acquisition of a dipole sonic and a density log from target to very near the Kelly bushing.

ACKNOWLEDGEMENTS

We thank the sponsors of the CREWES project for their support. Suncor is gratefully acknowledged for permission to use the logs and VSP data and for permission to publish these results. This work was funded by CREWES industrial sponsors and NSERC (Natural Science and Engineering Research Council of Canada) through the grant CRDPJ 461179-13.

REFERENCES

Aki, K, and P.G. Richards, 2002, Quantitative Seismology, University Science Books.

Ganley, D. C., 1981, A method for calculating synthetic seismograms which include the effects of absorption and dispersion, GEOPHYSICS Aug 1981, Vol. 46, No. 8, pp. 1100-1107.

Hauge, P. S., Measurements of attenuation from vertical seismic profiles, Geophysics, **48**, 1548-1558.

Kjartansson, E, 1979, Constant Q-wave Propagation and Attenuation, Journal of Geophysical Research, **84**, 4737-4748.

Margrave, G. F., 2013, Q tools: Summary of CREWES software for Q modelling and analysis, CREWES Research Report, Volume 25.

Margrave, G. F., 2014a, Stratigraphic filtering and Q estimation, CREWES Research Report, Volume 26.

Margrave, G. F., 2014b, VSP modelling in 1D with Q and buried source, CREWES Research Report, Volume 26.

O'Doherty, R. F., and N. A. Anstey, 1971, Reflections on Amplitudes, Geophysical Prospecting, 19, pp. 430-458.

Richards, P. G., and W. Menke, 1983, The apparent attenuation of a scattering medium: Bulletin of the Seismological Society of America, 73, 1005-1021.